Articles

Spectral Changes of Lignin Peroxidase during Reversible Inactivation†

Guojun Nie and Steven D. Aust*

Biotechnology Center, Utah State University, Logan, Utah 84322-4705

Received October 15, 1996; Revised Manuscript Received January 7, 1997⊗

ABSTRACT: The heme environment of lignin peroxidase (LiP) has been investigated by electronic absorption and electron paramagnetic resonance (EPR) spectroscopy. Native LiP was a pentacoordinate, high-spin ferric iron with a high-spin absorption band at 634 nm and *g* values at 5.86 and 2.07 in the EPR spectrum. Upon thermal inactivation, calcium ions were released from the enzyme and the Soret absorption decreased and red-shifted about 2 nm, the high-spin absorption band at 634 nm disappeared, and a low-spin absorption band appeared at 532 nm. The EPR spectrum and the temperature dependence of electronic absorption spectra revealed that the heme iron of the thermally inactivated enzyme was a mixture of high- and low-spin states, which was further supported by the changes in the electronic absorption and EPR spectra when cyanide was added to the thermally inactivated enzyme. Addition of various imidazoles or CN^- to thermally inactivated enzyme demonstrated that the low-spin heme iron of inactivated enzyme was hexacoordinate with a distal histidine as its sixth ligand, in contrast to the active enzyme, which was pentacoordinate and high-spin. Upon addition of calcium to recover the thermally inactivated LiP, the reactivated enzyme had absorptions at 408, 502, and 634 nm and *g* values at 5.86 and 2.07 in the EPR spectrum, which demonstrated that the heme iron of the reactivated enzyme was again high-spin and pentacoordinated.

Lignin peroxidase isozymes (LiP)[1] isolated from the white-rot fungus *Phanerochaete chrysosporium* are heme proteins with molecular weights from 38 000 to 42 000 and with p*I* values from 3.3 to 4.7 (Tien, 1987; Farrell et al., 1989). These isozymes catalyze the H_2O_2-dependent oxidation of lignin and lignin model compounds by the initial formation of an aryl cation radical with subsequent nonenzymatic reactions yielding a final product (Tien, 1987; Kirk & Farrell, 1987). It has also been found that the degradation of several xenobiotics involves LiP (Barr & Aust, 1994; Mileski et al., 1988; Bumpus & Brock, 1988; Sanglard et al., 1986; Haemmerli et al., 1986; Hammel et al., 1986, 1988; Schremer et al., 1988). Additionally, many compounds oxidized by LiP have high redox potentials, beyond the reach of plant peroxidases (Gold et al., 1989; Kirk & Farrell, 1987). This unique feature of LiP enables *P. chrysosproium* to degrade a variety of aromatic pollutants (Hammel, 1989; Valli & Gold, 1991). Therefore, *P. chrysosporium* has been applied to the biological treatment of wood pulp, waste water, and contaminated soil (Chung & Aust, 1995; Tien, 1987; Kirk, 1987).

Previous studies have demonstrated that the heme environment in native, resting LiP is similar to that of horseradish peroxidase (HRP) (deRopp et al., 1991; Kuila et al., 1985; Andersson et al., 1987; Mylrajun et al., 1990), cytochrome *c* peroxidase (CcP) (Banci et al., 1993; Poulos et al., 1993; deRopp et al., 1991), manganese peroxidase (MnP) (Banci et al., 1993; Wariishi et al., 1988; Sundaramoorthy, 1994), and *Arthromyces ramosus* peroxidase (Banci et al., 1993; Kunishima et al., 1994). These enzymes contain high-spin ferric iron in protoporphyrin IX. The heme iron is pentacoordinated (Kuila et al., 1985; Andersson et al., 1987) with a histidine as its fifth ligand, which is normally referred to as the "proximal" histidine in the proximal pocket. Another histidine on the other side of the heme plane is referred to as the "distal" histidine in the distal pocket. Both the distal and proximal histidines have been proposed to be involved in the mechanism of peroxidase catalytic cycle. In this mechanism, the distal histidine functions as acid−base catalyst to accept one proton from the incoming peroxide while the proximal histidine functions to stabilize the higher oxidation states of the heme iron atom by H-bond interaction with a nearby buried Asp (Poulos et al., 1993).

Calcium exists in many peroxidases (Sutherland & Aust, 1996; Haschke & Freidhoff, 1978; Maranon et al., 1993; Kunishima et al., 1994; Poulos et al., 1993; Sundaramoorthy et al., 1994). A role for calcium has been proposed to maintain the heme microenvironment and stabilize enzyme activity (Iori et al., 1995; Ogawa et al., 1979; Shiro et al., 1986; Maranon et al., 1993; Sundaramoorthy et al., 1994). We recently demonstrated that the loss of enzyme activity in LiP was due to the loss of calcium during thermal inactivation (Nie & Aust, 1997). The apparent inactivation rate could be decreased by addition of calcium and increased by Ca^{2+} chelators and the thermally inactivated LiP could be readily recovered upon addition of Ca^{2+}. We also reported that removal of calcium from LiP changed the heme environment and spin state of heme iron. Thermally inactivated LiP still contained one calcium, which might be

† This research was supported in part by Stockhausen GmbH and Co. KG, P.O. Box 570, D-47705/Krefeld 1, Germany.

* To whom correspondence should be addressed.

⊗ Abstract published in *Advance ACS Abstracts,* April 1, 1997.

[1] Abbrevations: LiP, lignin peroxidase; EGTA, ethylene glycol bis-(β-aminoethyl ether)-*N*,*N*,*N*′,*N*′-tetraacetic acid; EPR, electron paramagnetic resonance; CcP, cytochrome *c* peroxidase; HRP, horseradish peroxidase.

S0006-2960(96)02583-4 CCC: $14.00

the proximal calcium (in the proximal site of the heme pocket) since it was more tightly bound to LiP than the distal calcium (in the distal site) (Poulos et al., 1993). Therefore, the loss of the distal calcium may change the heme environment and spin state of heme iron and result in enzyme inactivation.

Of particular interest is one distal calcium ligand, Asp 48, which is bidentate bound to calcium, present in the distal helix (Poulos et al., 1993). The distal histidine, His 47, exists in the distal helix, adjacent to Asp 48 (Poulos et al., 1993). Upon removal of the distal calcium, Asp 48 may no longer be ligated, which may render the distal helix more flexible. Therefore, His 47 could bind the heme iron and finally inactivate the enzyme.

In this study, electronic absorption and EPR spectroscopy were utilized to investigate the changes in the heme environment, especially the spin and the coordination states of ferric iron of LiP during reversible inactivation, with particular interest in ligation on the distal side upon thermal inactivation.

MATERIALS AND METHODS

Chemicals. Hydrogen peroxide was purchased from Sigma Chemical Co. (St. Louis, MO). Veratryl alcohol, calcium chloride, imidazole, histidine methyl ester, 1-methylimidazole, 2-imidazolidone, and benzimidazole were purchased from Aldrich Chemical Co. (Milwaukee, WI). Tris(hydroxymethyl)aminomethane (Tris) and potassium cyanide were purchased from Mallinckrodt (Paris, KY). All buffers and solutions were prepared in purified water (Barnstead NANOpure II system, specific resistance 18.0 $M\Omega$ cm^{-1}) and all buffers were passed through a column of Chelex 100 (Bio-Rad, Richmond, CA).

Enzyme Preparation. Lignin peroxidases were produced and purified from extracellular fluid of cultures of *P. chrysosporium* as previously described (Tuisel et al., 1990). Lignin peroxidase isozyme H8, the isozyme used in this study, was further identified by analytical isoelectric focusing (Sutherland et al., 1996). Enzyme concentration was quantified using the extinction coefficient 169 mM^{-1} cm^{-1} at 408 nm (Tien et al., 1986). The veratryl alcohol oxidase activity of LiP was measured by the formation of veratryl aldehyde using conditions previously described (Nie & Aust, 1997). Thermal inactivation of LiP was carried out by placing enzyme mixtures in a plastic vial in a water bath at 51 °C (±0.5 °C). The reactivated enzyme was prepared by adding $CaCl_2$ to the thermally inactivated enzyme solution at 25 °C (Nie & Aust, 1997).

Spectral Characterization. Electronic absorption spectra were recorded on a UV-2101PC spectrophotometer (Shimadzu Scientific Instruments Inc., Columbia, MD) at the desired temperatures using quartz cuvettes of 1 cm light path, a slit width of 0.5 nm, and a scan speed of 18 nm/s. Temperature was thermostatically controlled and recorded in the reference cuvette using a digital thermometer 800 (VWR Scientific, San Francisco, CA).

EPR Spectroscopy. Low-temperature (4 K) EPR spectra were obtained with a Bruker ESP 300 spectrometer equipped with an Oxford ESR 10 helium-flow cryostat and DTC-2 temperature controller. The enzymes were concentrated by using Centricon-10 concentrators (Amicon, Inc., Beverly, MA). EPR g values were calculated from field strengths determined by a frequency counter RS 232 and were estimated to be accurate to 0.01 unit.

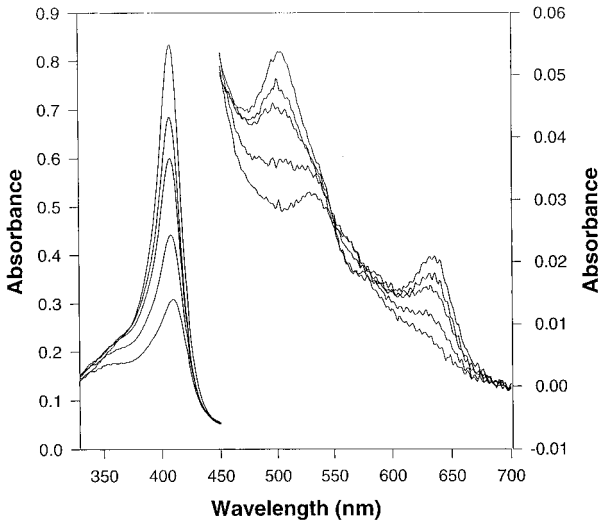

FIGURE 1: Absorption spectra of LiP during thermal inactivation. Thermal inactivation of LiP H8 was carried out in a plastic vial containing 3.3 μM enzyme and 20 mM Tris-HCl buffer, pH 7.9, in a water bath at 51 °C. Aliquots of the enzyme mixture were taken and absorption spectra were recorded in a cuvette at 25 °C after 0, 4, 7, 18, and 50 min, top to bottom, at a scan speed of 18 nm/s. The corresponding activity remaining was 100%, 74.7%, 57.5%, 24%, and 0%, again, top to bottom.

RESULTS

Figure 1 shows the electronic absorption spectra of LiP H8 during thermal inactivation. As the incubation time increased, the Soret absorbance decreased and finally was 37% that of active enzyme. In addition, the Soret band red-shifted from 408 nm in the active enzyme to 410 nm in the inactivated form and a weak absorption at 359 nm concomitantly appeared (Figure 1, Table 1). Moreover, the absorption spectra changed markedly at higher wavelength during thermal inactivation. The absorptions at 634 and 502 nm disappeared and absorption at 532 nm concomitantly appeared (Figure 1, Table 1). Isobestic points were observed at 442, 544, and 583 nm, suggesting that enzyme structural changes occurred with no obvious intermediates.

When cyanide was added to active LiP, the Soret band red-shifted from 408 to 422 nm and new bands at 359 and 542 nm appeared with concomitant disappearance of the bands at 502 and 634 nm (Figure 2A). When cyanide was added to thermally inactivated LiP, the Soret band again red-shifted from 410 to 420 nm and the band at 532 nm red-shifted to 541 nm (Figure 2B). Additionally, the absorption was further decreased at 634 nm. Although the absorption spectra of the cyanide adducts of active and inactive enzymes were similar, the extinction coefficient of the Soret in the inactive enzyme was lower than that of active enzyme (Figure 2, Table 1). This indicated that the heme environments of the active and thermally inactivated LiP were different. Absorptions at 359 and 532 nm suggested that the heme iron of thermally inactivated LiP was a low-spin state or a mixture of high- and low-spin states.

Temperature-dependent changes in the absorption spectrum of thermally inactivated LiP were observed (data not shown). The Soret band blue shifted from 410 to 396 nm and decreased as the temperature was raised from 5 to 56

Table 1: Electronic Absorption Parameters of LiP[a]

enzyme	δ[b]	Soret	CT_2[c]	β	α	CT_1
LiP		408 (168)	502 (13)			634 (4.7)
LiP-CN	359 (40)	422 (108)		542 (12)		
inactive LiP	359 (53)	410 (63)		532 (8.3)	562 (s)[d]	
inactive LiP-CN	362 (40)	420 (77)		541 (9.4)	562 (s)	
inactive LiP-Im	359 (35)	411 (109)		533 (9.4)		

[a] Absorption maxima are in nanometers; the millimolar extinction coefficients are given in parentheses. All absorption spectra were recorded at pH 7.9 and 25 °C. [b] δ, Soret, CT_2, β, α, and CT_1 denote the type of the absorption band. [c] Charge-transfer bands. [d] s deontes a shoulder on a major peak.

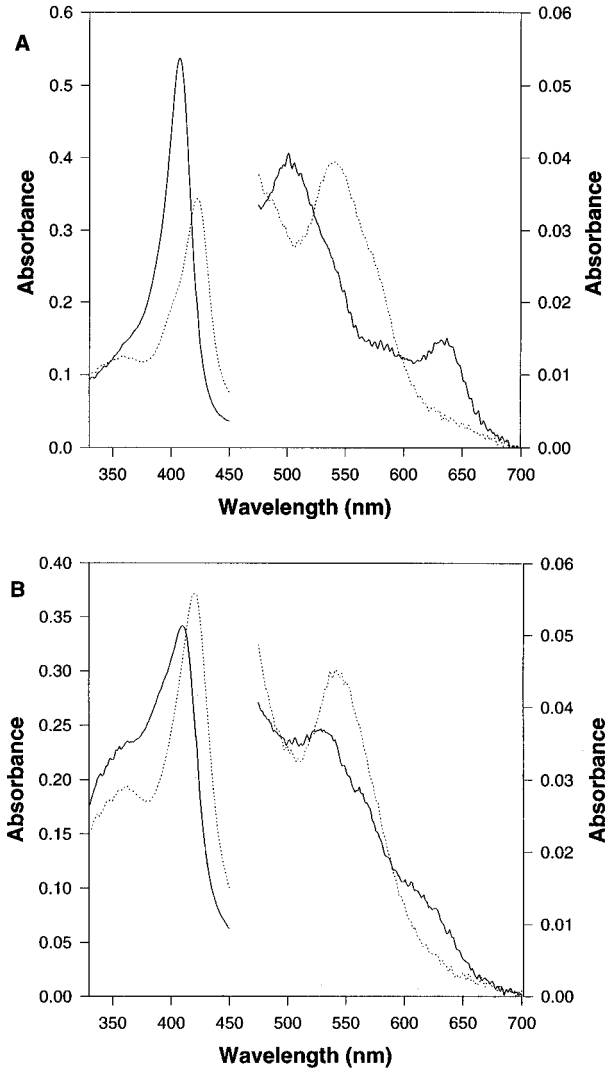

FIGURE 2: Absorption spectra of cyanide derivatives of active and thermally inactivated LiP. (A) Absorption spectra of active LiP, 3.2 μM in 2 mM Tris-HCl buffer, pH 7.9, in the absence (—) and presence (···) of 5 mM potassium cyanide. (B) Absorption spectra of thermally inactivated LiP, 4.8 μM, in 20 mM Tris-HCl buffer, pH 7.9, in the absence (—) and presence (···) of 5 mM potassium cyanide. Thermally inactivated LiP was prepared as described in Figure 1 to less than 2% of original activity.

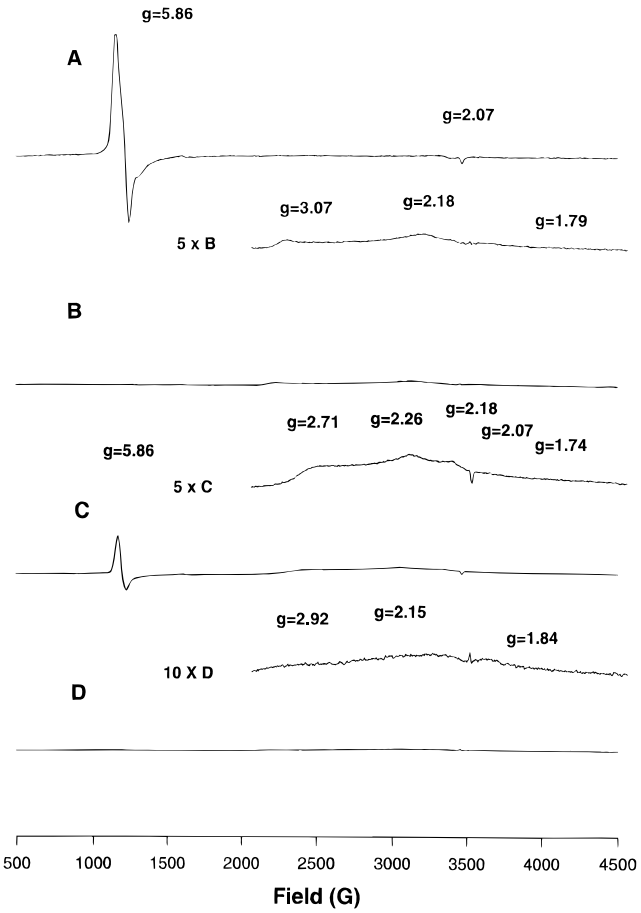

FIGURE 3: EPR spectra of active and inactivated LiP and their cyanide adducts at 4 K. (A) Active LiP; (B) active LiP in the presence of 20 mM potassium cyanide; (C) inactivated LiP; (D) inactivated LiP in the presence of 20 mM potassium cyanide. All samples contained 200 μM LiP in 20 mM Tris-HCl buffer, pH 7.9. Inactivated LiP was prepared as described in Figure 1 to less than 2% of original activity. Spectral acquisition conditions were as follows: temperature, 4 K; microwave frequency, 9.65 GHz; microwave power, 0.10 mW; modulation amplitude, 5 G; modulation frequency, 100 kHz; time constant, 10.24 ms; scan time, 10.49 s; gain, 1×10^4.

°C. Additionally, the intensity of the high-spin band at 634 nm increased and that of the low-spin band at 532 nm decreased. These results are also indicative of a thermally sensitive mixture of high- and low-spin states of inactivated LiP. However, the spectrum of active LiP was insensitive to changes in temperature between 5 and 56 °C (data not shown).

The EPR spectra of active and inactivated LiP and their cyanide adducts are shown in Figure 3 and EPR *g* values of these enzymes are listed in Table 2. The *g* values for active LiP at 5.86 and 2.07 are characteristic of a high-spin pentacoordinate ferric heme (Figure 3A, Table 2), whereas the *g* values for the cyanide adduct at 3.07, 2.18, and 1.79 represent a low-spin hexacoordinate ferric heme (Figure 3B, Table 2). These *g* values are quite consistent with the results previously reported (Andersson et al., 1985). In the EPR spectrum of thermally inactivated LiP, both ferric high-spin signals at $g = 5.86$ and 2.07 and the low-spin signals at $g =$ 2.71, 2.22, 2.18, and 1.74 were observed (Figure 3C, Table 2). However, the intensities of the high-spin signals of inactivated LiP were 29% those of active enzyme. These

Table 2: EPR *g* Values of LiP[a]

enzyme	*g* values[b]					
LiP	5.86	2.07				
LiP-CN	3.07	2.18	1.79			
inactive LiP	5.86	2.71	2.26	2.18	2.07	1.74
inactive LiP-CN	2.92	2.5	1.84			
inactive LiP-imidazole	5.88	2.87	2.26	1.80		
recovered LiP	5.86	2.07				

[a] All EPR spectra were recorded at 4 K and pH 7.9. [b] *g* values were calculated from field strengths and estimated to be accurate to ±0.01 unit.

support the conclusion that thermally inactivated LiP was a mixture of high- and low-spin states. The mixed spin states of inactivated LiP were completely converted to low-spin upon addition of cyanide (Figure 3D). This result also suggested that the sixth iron ligand of the thermally inactivated LiP was replaced by cyanide.

Upon addition of imidazole, the Soret absorbance increased and shifted from 410 to 411 nm (Figure 4A, Table 1). Additionally, the absorbance at 532 nm increased and that at 634 nm further decreased. These results suggested that the distal His 47 was the sixth iron ligand in inactivated LiP. However, the His 47 must be loosely bound to the heme iron because the absorption of the Soret increased upon addition of imidazole. Titration of heme with imidazole increased the Soret absorbance in addition to the red shift, and the final spectrum of bisimidazole heme model complex had a Soret band at 413 nm (Figure 4B), which was in good agreement with the previous reports (Desbois & Lutz, 1992). These results suggested that the heme iron was a bisimidazole in inactivated LiP. However, imidazole did not affect the absorption spectrum of active LiP (data not shown).

The absorption maxima of inactivated LiP in the presence of a variety of exogenous nitrogen ligands are given in Table 3. 1-Methylimidazole and histidine methyl ester were as good as imidazole as the sixth iron ligand. Benzimidazole did not affect the absorption spectrum of inactivated LiP (Table 3). However, this may be explained by the fact that benzimidazole is bulkier than 1-methylimidazole and histidine methyl ester. Additionally, the benzene ring of benzimidazole is rigid. Therefore, it must not have entered the small heme pocket to ligate the heme iron. 2-Imidazolidone also did not interact with the heme iron of inactivated LiP, presumably because it lacks the unsaturated bound nitrogen. These results further indicated that the distal histidine was the sixth iron ligand.

Upon addition of cyanide to the inactive enzyme previously complexed with imidazole, the final spectrum was similar to that of the direct adduct of cyanide to inactivated LiP (Figures 2B and 5). These data indicate that the heme was not free and imidazole just replaced the distal histidine after imidazole was added to the inactivated LiP. However, cyanide addition did not further decrease the absorbance at 634 nm, suggesting that imidazole enhanced the conversion of high-spin to low-spin state of inactivated LiP.

The intensity of the high-spin EPR signal of inactivated LiP further decreased to 18%, as imidazole ligated to the heme iron (Figure 6). This result was quite consistent with changes in the higher wavelength region of the absorption spectra as imidazole was added to thermally inactivated LiP, but it was in contrast to the increased absorbance as the Soret band (Figure 4A). However, the increased absorbance of the Soret band in inactivated LiP was consistent with the

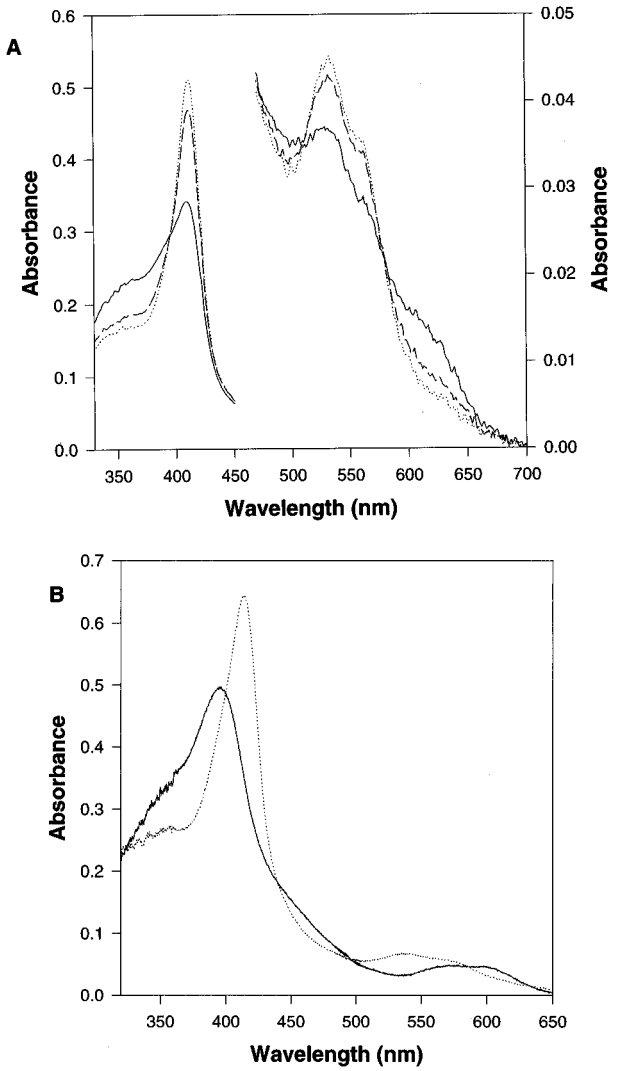

FIGURE 4: Absorption spectra of imidazole derivatives of thermally inactivated LiP and heme. (A) Absorption spectra of thermally inactivated LiP (4.8 μM) were recorded in 20 mM Tris-HCl buffer, pH 7.9, in the presence of no imidazole (—), 5 mM imidazole (- - -); or 15 mM imidazole (•••). The thermally inactivated LiP was prepared as described in Figure 1 to less than 2% of original activity. (B) Absorption spectra of heme (100 μM) were recorded in 20 mM Tris-HCl buffer, pH 7.9, and 2% cationic detergent cetyltrimethylammonium bromide, in the presence of no imidazole (—) or 50 mM imidazole (•••).

Table 3: Electron Absorption Parameters of LiP with Various Nitrogen Ligands[a]

enzyme	δ[b]	Soret	β	α
inactive LiP	359 (53)	410 (63)	532 (8.2)	562 (s)[c]
1-methylimidazole-inactive LiP	359 (36)	412 (102)	531 (10.1)	562 (s)
histidine methyl ester-inactive LiP	357 (35)	411 (101)	531 (9.2)	564 (s)
benzimidazole-inactive LiP[d]				
2-imidazolidone-inactive LiP[d]				

[a] Absorption maxima are in nanometers; the millimolar extinction coefficients are given in parentheses. All absorption spectra were recorded at pH 7.9 and 25 °C. [b] δ, Soret, CT_2, β, and α denote the type of absorption band. [c] (s) denotes a shoulder on a major peak. [d] No obvious spectral changes were observed after this chemical was added.

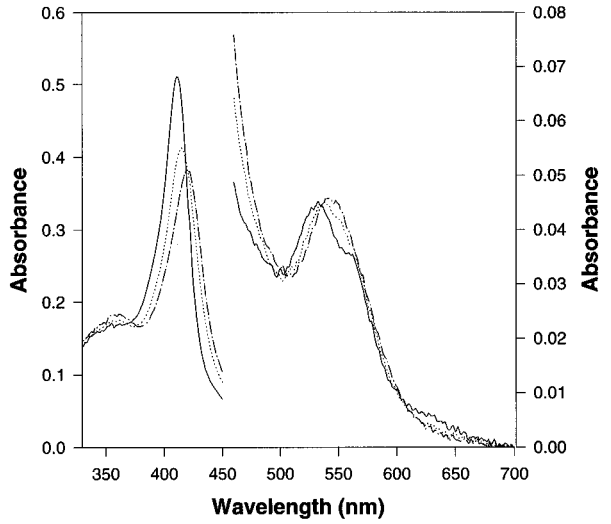

FIGURE 5: Effect of cyanide on the absorption spectrum of the imidazole complex of thermally inactivated LiP. The spectra were recorded in 20 mM Tris-HCl buffer, pH 7.9, in the presence of no cyanide (—), 5 mM cyanide (•••), or 10 mM cyanide (— • —). The thermally inactivated LiP imidazole complex was prepared by adding 15 mM imidazole to the thermally inactivated LiP (4.8 μM), prepared as described in Figure 1 to less than 2% of original activity.

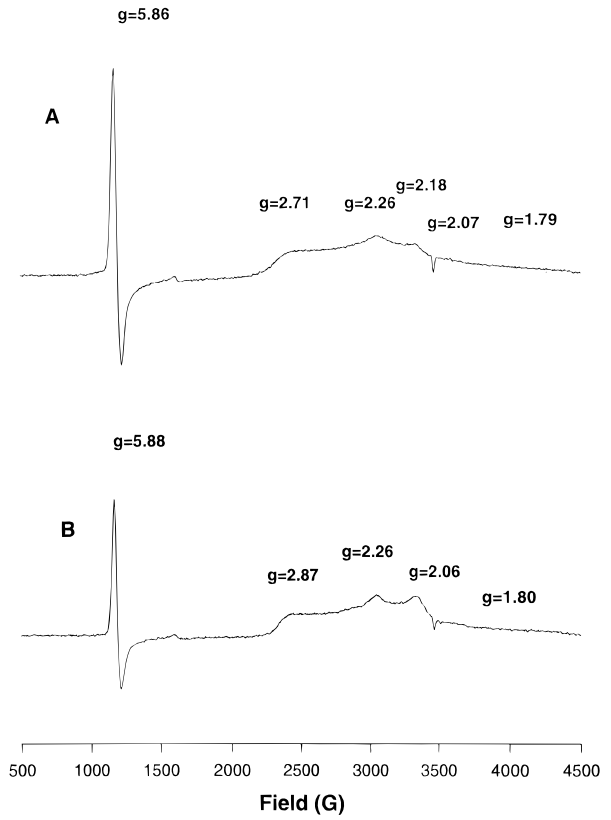

FIGURE 6: EPR spectra of thermally inactivated LiP and its imidazole complex at 4 K. (A) Inactivated LiP; (B) inactivated LiP in the presence of 20 mM imidazole. All samples contained 200 mM LiP in 20 μM Tris-HCl buffer, pH 7.9. Enzyme preparations were described in Figures 1 and 5. Spectral acquisition conditions were described in Figure 4.

increased Soret absorbance of model heme when symmetric bisimidazole heme was formed upon addition of imidazole to the heme. The increased symmetry of heme iron due to exogenous imidazole ligation was reflected by the decreased high-spin signal intensities.

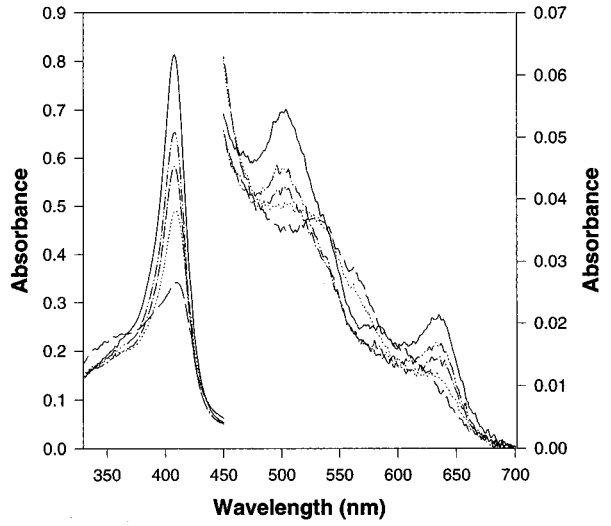

FIGURE 7: Absorption spectra of LiP during reactivation. Enzyme inactivation to less than 2% of original activity was as described in Figure 1. Reactivation was carried in a plastic vial containing 4.8 μM enzyme and 20 mM Tris-HCl buffer, at 25 °C. The spectra were recorded at 0 (- - -), 0.5 (•••), 4 (— • —), and 20 h (— •• —), under the same conditions as described in Figure 1. The corresponding recovered activities were 2.6%, 31.8%, 68.1%, and 82.4%. The absorption spectrum of the initial active LiP (—) is also shown.

The Soret band gradually blue-shifted from 410 to 408 nm, concomitantly with the increased absorbance after calcium was added to thermally inactivated LiP (Figure 7). Additionally, the low-spin absorption band at 532 nm disappeared and the high-spin absorption bands at 502 and 634 nm reappeared. The reactivated enzyme had the same absorbance maxima at 408, 502, and 634 nm as the original active LiP. Isosbestic points were observed at 425, 473, and 613 nm, which were different from those during thermal inactivation, suggesting that enzyme inactivation and reactivation may have different pathways. The EPR spectrum of reactivated LiP had signals at *g* values identical to those of active LiP.

DISCUSSION

We recently reported that the thermal inactivation of LiP was due to the loss of calcium from LiP causing changes in the heme environment (Nie & Aust, 1997). However, the detailed changes in the heme environment were not characterized. In this study, electronic absorption and EPR spectroscopy were utilized to provide complementary information on the coordination and spin state of ferric iron of LiP during reversible inactivation. Thermally inactivated LiP had absorption at 359, 410, 532, and 562 nm, in sharp contrast to active LiP, with absorption bands at 408, 502, and 634 nm, which are characteristic of a high-spin pentacoordinate ferric heme protein (Andersson et al., 1985, 1987). These data indicated a change of heme iron from a pentacoordinated high-spin to hexacoordinated low-spin (Hollenberg et al., 1980; Yonetani et al., 1966), which was supported by several lines of evidence. First, the absorption spectrum of inactivated LiP was similar to that of the cyanide adduct of active LiP in the higher wavelength region, suggesting that inactivated LiP was hexacoordinated low-spin because the heme iron of the cyanide adduct of active LiP is hexacoordinated low-spin with cyanide as its sixth ligand (Andersson et al., 1985). The spectral differences also indicated that the inactivated LiP was not entirely hexa-

coordinated low-spin. This was confirmed by the spectrum of cyanide adduct of inactivated LiP. These changes implied that an unknown ligand became the sixth ligand in thermally inactivated LiP and could be replaced by cyanide.

The proposed mixed spin states were further confirmed by the temperature-dependent spectra of inactivated LiP, which also suggested that the heme pocket of inactivated LiP may be more flexible than that of active LiP and the sixth ligand just loosely bound the heme iron. Further evidence came from the low-temperature EPR spectra, which clearly demonstrated that the inactivated LiP was mixed low- and high-spin with the low-spin state being predominant. The mixed spin states indicated a mixture of penta- and hexa-coordinated heme or a loosely bound sixth ligand to the iron.

X-ray crystallography indicated that the heme iron of active LiP was pentacoordinate with histidine as the proximal fifth ligand and that the distal His 47 was too far away from the heme iron to serve as a sixth ligand (Poulos et al., 1993). They also reported that two calcium ions existed in the enzyme structure to maintain the heme environment. The distal calcium was predicted to be more loosely bound to protein compared to the proximal calcium (Poulos et al., 1993). We recently reported that all but one calcium was removed from the 5 mol of calcium in native LiP during thermal inactivation (Nie & Aust, 1997). Therefore, we proposed that the distal calcium was lost during inactivation. One of the distal calcium ligands, Asp 48, is in the distal helix and His 47 is immediately adjacent in the same helix (Poulos et al., 1993). Upon removal of the distal calcium, Asp 48, was no longer ligated, which may greatly affect the conformation of the distal helix and account for the sensitivity to temperature of thermally inactivated LiP. We propose that His 47 might bind the heme iron as a sixth ligand, rendering LiP inactive. If His 47 is the sixth iron ligand, it might be replaced by imidazole. Indeed, both the increased absorbance and a red shift to 411 nm in the Soret were observed when imidazole was added to thermally inactivated LiP, suggesting that distal histidine was the sixth ligand of inactivated LiP. Addition of other nitrogen ligands to thermally inactivated LiP further supported this conclusion. Although the distal His 47 was the sixth iron ligand in inactivated LiP, it did not bind the ferric iron in active LiP (Poulos, 1993). However, distal His 52 CcP could bind the heme iron as a sixth ligand at alkaline pH even though the distal His was approximately the same distance from the heme iron in LiP and CcP, 5.3 and 5.5 Å, respectively (Finzel et al., 1984; Poulos et al., 1993). The distal His binding in CcP resulted in formation of a low-spin bisimidazole complex with an absorption spectrum similar to that of thermally inactivated LiP, with absorption at ~533 and 563 nm (Smulevich et al., 1991). This difference between LiP and CcP may be explained by the fact that CcP does not contain calcium to maintain the heme environment as does LiP (Poulos et al., 1980, 1993).

Upon removal of the distal calcium from MnP, the distal histidine could bind the heme iron as a sixth ligand (Sutherland et al., 1996, 1997). A mutation designed to decrease the binding affinity for distal calcium in MnP (D47A) had no enzyme activity (Sutherland et al., 1997). The absorption spectrum of thermally inactivated LiP was similar to that of the D47A mutant of MnP, with absorption at 359, 412, 533, and 561 nm, indicating that the distal calcium was important for maintaining the heme environment. Upon removal of all calcium from HRP, the enzyme was still 40% active (Haschke & Friedhoff, 1978) and the heme iron was changed from high-spin to low-spin (Shiro et al., 1986). The change in the spin state of HRP was most probably due to the proximal imidazole whose changed binding nature was induced by removal of calcium from the enzyme (Shiro et al., 1986). However, the major reason for the spin-state change in LiP was that His 47 bound the iron, resulting in an increased axial symmetry. Although removal of calcium from cationic peanut peroxidase (CPP) caused a 2-fold decrease in enzyme activity (van Huystee et al., 1992), the absorption spectrum and spin state of heme iron did not significantly change (Maranon et al., 1993, 1994). However, this particular phenomenon could be explained by the recently solved crystal structure of CPP. One disulfide bound found in the distal side of CPP forms a loop encompassing several of the distal calcium ligands (Schuller et al., 1996). The conformation of the distal helix might therefore by maintained by the disulfide as the distal calcium is removed.

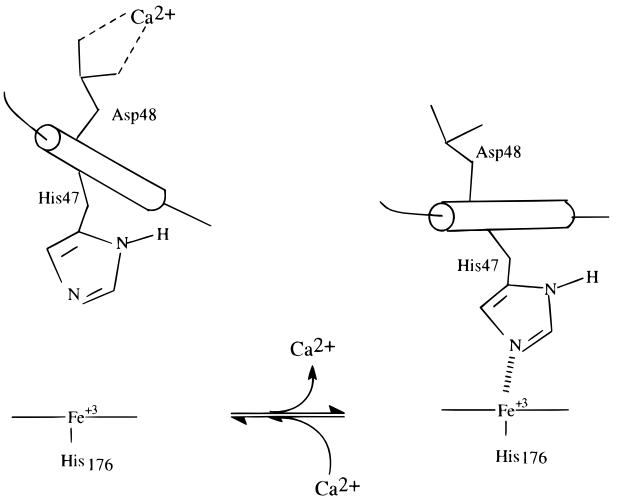

FIGURE 8: Proposed scheme for the structural changes of heme environment of LiP during reversible inactivation. The distal helix is represented as a cylinder. His 47 and Asp 48 are in this helix. Active enzyme is pentacoordinated and inactive enzyme is hexa-coordinated, with His 47 providing the additional coordination.

In conclusion, although 5 mol of calcium was found in our enzyme preparation, only two calcium binding sites were located by crystal structural analysis, which suggested that other calcium ions might be even much loosely bound than the distal calcium. Therefore, it is assumed that removal of the very loosely bound calcium may not contribute to the spectroscopic changes and the distal calcium may plays an important role in the coordination and spin state of heme iron in LiP. Removal of the distal calcium may leave Asp 48 free in the distal helix, resulting in the distal helix being more flexible. Therefore, the distal His 47 in the helix could bind the heme iron as the sixth ligand, which changed the spin state of heme iron and inactivated the LiP. A scheme is shown in Figure 8 to illustrate the proposed structural changes occurring in the heme environment of LiP during reversible inactivation. Other structural changes were also observed by circular dichroism of active and thermally inactivated LiP (Sutherland et al., 1997). Although the distal calcium had a profound effect on the coordination and spin state of heme iron, additional work will be done to elucidate further overall structural changes during thermal inactivation.

ACKNOWLEDGMENT

We thank Terri Maughan for preparing the manuscript, Greg R. J. Sutherland for helpful discussion, and Yixin Ben for production of LiP from *P. chrysosporium*.

REFERENCES

Andersson, L. A., Renganathan, V., Chiu, A. A., Loehr, T. M., & Gold, M. H. (1985) *J. Biol. Chem. 260*, 6080−6087.

Andersson, L. A., Renganathan, V., Loehr, T. M., & Gold, M. H. (1987) *Biochemistry 26*, 2258−2263.

Banci, L., Bertini, I., Kuan, I.-C., Tien, M., Turano, P., & Vila, A. J. (1993) *Biochemistry 32*, 13483−13489.

Barr, D. P., & Aust, S. D. (1994) *Environ. Sci. Technol. 28*, 78A−87A.

Bumpus, J. A., & Brock, B. J. (1988) *Appl. Environ. Microbiol. 54* (5), 1143−1150.

Chung, N., & Aust, S. D. (1995) *J. Hazard. Mater. 41*, 177−183.

deRopp, J. S., LaMar, G. N., Wariishi, H., & Gold, M. H. (1991) *J. Biol. Chem. 266*, 15001−15008.

Desbois, A., & Lutz, M. (1992) *Eur. Biophys. J. 20*, 321−335.

Dunford, H. B., & Stillman, J. S. (1976) *Coord. Chem. Rev. 19*, 187−251.

Farrell, R. L., Murtagh, K. E., Tien, M., Mozuch, M. D., & Kirk, T. K. (1989) *Enzyme Microb. Technol. 11*, 322−328.

Finzel, B. C., Poulos, T. L., & Kraut, J. (1984) *J. Biol. Chem. 259*, 13027−13036.

Fukuyama, K., Kunishima, N., Amada, F., & Kubota, T. (1996) *J. Biol. Chem. 270*, 21884−21892.

Gold, M. H., Wariishi, H., & Valli, K. (1989) in *Biocatalysis in Agricultural Biotechnology* (Whitaker, J. R., & Sonnet, P., Eds.) ACS Symposium Series 389, pp 127−140, American Chemical Society, Washington, DC.

Haemmerli, S. D., Leisola, M. S. A., Sanglard, D., & Fiechter, A. (1986) *J. Biol. Chem. 261*, 6900−6903.

Hammel, K. E. (1989) *Enzyme Microb. Technol. 11*, 776−777.

Hammel, K. E., & Tardane, P. J. (1988) *Biochemistry 27*, 6563−6568.

Hammel, K. E., Kalyanaraman, B., & Kirk, T. K. (1986) *J. Biol. Chem. 261*, 16943−16952.

Haschke, R. H., & Freidhoff, T. M. (1978) *Biochem. Biophys. Res. Commun. 80*, 1039−1042.

Hollenberg, P. F., Hager, L. P., Blumberg, W. E., & Peisach, Y. (1980) *J. Biol. Chem. 255*, 4801−4807.

Iori, R., Cavalieri, B., & Palmieris, S. (1995) *Cereal Chem. 72*, 176−181.

Kirk, T. K. (1987) *Philos. Trans. R. Soc. London 321A*, 61.

Kirk, T. K., & Farrell, R. L. (1987) *Annu. Rev. Microbiol. 41*, 465−505.

Kuila, D., Tien, M., Fee, J. A., & Ondrias, M. R. (1985) *Biochemistry 24*, 3394−3397.

Kunishima, N., Fukuyama, K., & Matsuara, H. (1994) *J. Mol. Biol. 235*, 331−344.

Maranon, M. J. R., & van Huystee, R. B. (1994) *Photochemistry 37*, 1217−1225.

Maranon, M. J. R., Stillman, M. J., & van Huystee, R. B. (1993) *Biochem. Biophys. Res. Commun. 194*, 326−333.

Mileski, G. J., Bumpus, J. A., Jurek, M. A., & Aust, S. D. (1988) *Appl. Environ. Microbiol. 54*, 2885−2889.

Mylraya, M., Valli, K., Wariishi, H., Gold, M. H., & Loehr, T. M. (1990) *Biochemistry 29*, 9617−9623.

Nie, G., & Aust, S. D. (1997) *Arch. Biochem. Biophys. 337*, 225−231.

Ogawa, S., Shiro, Y., & Morishma, J. (1979) *Biochem. Biophys. Res. Commun. 90*, 674−678.

Poulos, T. L., Edwards, S. L., Wariishi, H., & Gold, M. H. (1993) *J. Biol. Chem. 268*, 4429−4440.

Sanglard, D., Leisola, M. S. A., & Fiechter, A. (1986) *Enzyme Microb. Technol. 8*, 209−212.

Schremer, R. P., Stevens, J. E., & Tien, M. (1988) *Appl. Environ. Microbiol. 54*, 1858−1860.

Schuller, D. J., Bean, N., van Huystee, R. B., McPherson, A., & Poulos, T. L. (1996) *Structure 4*, 311−321.

Shiro, Y., Kurono, M., & Isao, M. (1986) *J. Biol. Chem. 261*, 9382−9390.

Smulevich, G., Miller, M. A., Kraut, T., & Spiro, T. G. (1991) *Biochemistry 30*, 9546−9558.

Sundaramoorthy, M., Kishi, K., Gold, M. H., & Poulos, T. L. (1994) *J. Biol. Chem. 269*, 32759−32767.

Sutherland, G. R. J., & Aust, S. D. (1996) *Arch. Biochem. Biophys. 332*, 128−134.

Sutherland, G. R. J., Khindaria, A. & Aust, S. D. (1996) *Arch. Biochem. Biophys. 327*, 20−26.

Sutherland, G. R. J., Zapanta, L. S., Tien, M., & Aust, S. D. (1997) *Biochemistry 36*, 3654−3662.

Tien, M. (1987) *CRC Crit. Rev. Microbiol. 15*, 141−168.

Tien, M., Kirk, T. K., Bull, C., & Fee, J. A. (1986) *J. Biol. Chem. 261*, 1687−1693.

Tuisel, H., Sinclair, R., Bumpus, J. A., Ashbaugh, W., Brock, B. J., & Aust, S. D. (1990) *Arch. Biochem. Biophys. 279*, 158−166.

Valli, K., & Gold, M. H. (1991) *J. Bacteriol. 173*, 345−352.

van Huystee, R. B., Xu, Y., and O'Donnell, J. P. (1992) *Plant Physiol. Biochem. 30*, 293−297.

Wariishi, H., Akileswaran, L., & Gold, M. H. (1988) *Biochemistry 27*, 5365−5370.

Yonetani, T., Wilson, D. F., & Seamonds, B. (1996) *J. Biol. Chem. 241*, 5347−5352.

BI962583O